Contrib Mineral Petrol (1991) 108:463–471

Contributions to Mineralogy and Petrology

Oxygen diffusion in basalt and andesite melts: experimental results and discussion of chemical versus tracer diffusion

Richard F. Wendlandt

Department of Geology and Geological Engineering, Colorado School of Mines, Golden, CO 80401, USA

Received September 24, 1990 / Accepted April 8, 1991

Abstract. Chemical diffusion coefficients for oxygen in melts of Columbia River basalt (Ice Harbor Dam flow) and Mt. Hood andesite have been determined at 1 atm. The diffusion model is that of sorption or desorption of oxygen into a sphere of uniform initial concentration from a constant and semi-infinite atmosphere. The experimental design utilizes a thermogravimetric balance to monitor the rate of weight change arising from the response of the sample redox state to an imposed f_{O_2}. Oxygen diffusion coefficients are approximately an order-of-magnitude greater for basaltic melt than for andesitic melt. At 1260° C, the oxygen diffusion coefficients are:

$D = 1.65 \times 10^{-6}$ cm^2/s

and

$D = 1.43 \times 10^{-7}$ cm^2/s

for the basalt and andesite melts, respectively. The high oxygen diffusivity in basaltic melt correlates with a high ratio of nonbridging oxygen/tetrahedrally coordinated cations, low melt viscosity, and high contents of network-modifying cations. The dependence of the oxygen diffusion coefficient on temperature is:

$D = 36.4 \exp(-51{,}600 \pm 3200/RT)$ cm^2/s

for the basalt and

$D = 52.5 \exp(-60{,}060 \pm 4900/RT)$ cm^2/s

for the andesite (R in cal/deg-mol; T in Kelvin). Diffusion coefficients are independent of the direction of oxygen diffusion (equilibrium can be approached from extremely oxidizing or reducing conditions) and thus, melt redox state. Characteristic diffusion distances for oxygen at 1260° C vary from 10^{-2} to 10^2 m over the time interval of 1 to 10^6 years. A compensation diagram shows two distinct trends for oxygen chemical diffusion and oxygen tracer diffusion. These different linear relationships are interpreted as supporting distinct oxygen transport mechanisms. Because oxygen chemical diffusivities are generally greater than tracer diffusivities and their Arrhenius activation energies are less, transport mechanisms involving either molecular oxygen or vacancy diffusion are favored.

Introduction

Chemical diffusion of species in silicate melts may control the rate of numerous transport-related igneous processes including magma mixing, assimilation, fractional crystallization, and partial melting. Experimental investigations of diffusion in magmatic systems have dealt primarily with cationic species (see reviews by Hofmann 1980; Dunn 1986) and rarely with anionic components, including oxygen. The paucity of kinetic studies involving oxygen is surprising inasmuch as oxygen is the principal constituent of abundant igneous magmas and, therefore, its diffusional behavior should help explain other melt properties, including the rates and possibly the directions of cation diffusion (e.g., Davis and Pask 1972), melt structure, crystal growth and dissolution, and viscous flow.

Most of the existing work on oxygen diffusion has been done in simple binary and ternary systems (partially summarized by Dunn 1982; Schreiber et al. 1986). These experiments, generally designed to yield self-diffusion coefficients, have shown that there is a crude compositional control on oxygen diffusivity: melts rich in network-forming components, such as Si and Al, tend to have low oxygen diffusivities while those melts with high proportions of network-modifying cations, alkalis, in particular, have high diffusivities (Oishi et al. 1975). The alkali content of melts also generally correlates with diffusivity, although for similar temperatures and molar compositions, sodium-rich melts have oxygen self-diffusivities that are 2–3 times greater than those for potassic silicate melts (May et al. 1974; May and Wollast 1974). Dunn (1982) notes that the range of oxygen diffusivities in silicate melts corresponds to the observed range of divalent

cation diffusivities and that oxygen conforms to the compensation law for cation diffusion. On the basis of these observations, he suggests that oxygen diffusion mechanisms might resemble those for cation diffusion and involve, at least in part, discrete O^{2-} anions. Schreiber et al. (1986) however, propose that diffusion mechanisms for tracer and chemical diffusion are different, the former involving anionic oxygen species and interactions between oxygen and network-forming aluminosilicate anions and the latter involving molecular oxygen. Although May et al. (1974) and May and Wollast (1974) reported oxygen diffusivities, D, varying inversely with partial pressure of oxygen, subsequent measurements (Muehlenbachs and Kushiro 1974; deBerg and Lauder 1978, 1980, Wendlandt 1980, this study; Schreiber et al. 1986) have indicated that D is independent of the oxidation state of the system.

In this investigation, chemical diffusion coefficients are reported for oxygen in natural basaltic and andesitic melts. There are few other studies of oxygen diffusion in natural silicate systems. Muehlenbachs and Kushiro (1974) and Canil and Muehlenbachs (1990) reported tracer diffusion coefficients at 1 atm for a basaltic melt of unspecified composition and an iron-rich basalt from the Galapagos spreading center, respectively. Chemical diffusion coefficients have been determined for Hamada nephelinite, 1921 Kileaua tholeiite, and alkali olivine basalt melts at elevated pressures (Dunn 1983), andesite melt as a function of pressure at 1350° C (Dunn and Scarfe 1986), and Columbia River basalt and Mt. Hood andesite melt at one atmosphere (Wendlandt 1980). The differences between self and chemical diffusion have been discussed elsewhere (e.g., Hofmann 1980; Dunn 1986). From the perspective of this study, the principal disadvantage of chemical diffusion studies is that chemical potential gradients impose compositional effects on the diffusion coefficients resulting in measured effective diffusivities that may be rigorously applicable only when the experimental end-points are matched by those in nature. The advantage of these types of experiments, however, is that many processes involving silicate melts are mass transport processes and, perhaps, best constrained by chemical diffusion measurements.

Table 1. Melt compositions

Oxide	Prerun		Postrun		
	GIB	MHA	GIB	GIB-2	MHA
Weight percent					
SiO_2	45.93	60.78			61.39
TiO_2	3.73	0.83			0.85
Al_2O_3	11.67	17.38			18.23
Fe_2O_3	4.06	2.24			
FeO	13.36	3.38	17.7	16.5	5.49
MnO	0.30	0.10			0.13
MgO	4.23	3.12			3.41
CaO	8.81	6.09			6.39
Na_2O	2.40	4.16	1.36	1.53	2.13
K_2O	1.28	1.20			0.81
P_2O_5	1.77	0.18			
S	0.13	n.d.			
H_2O_t	1.03	0.44			
	98.70	99.90			98.83
Cations per 100 oxygens					
Si	29.30	34.66			
Ti	1.79	0.36			
Al	8.78	11.69			
Fe^{3+}	1.95	0.96			
Fe^{2+}	7.13	1.61			
Mn	0.16	0.05			
Mg	4.02	2.65			
Ca	6.02	3.72			
Na	2.97	4.60			
K	1.04	0.87			
P	0.96	0.09			
NBO/T	0.898	0.274			
Network modifying cations	23.29	14.46			

Analyses completed at the Johnson Space Center, Houston, TX. Prerun: total H_2O by ignition; Na_2O by INAA; FeO by titration; other elements by XRF; n.d., not determined. Postrun: sodium and iron by INAA (GIB, GIB-2); MHA analyzed by electron microprobe

NBO/T = nonbridging oxygen/tetrahedrally coordinated cations (Si, Ti, Al, P) (Mysen et al. 1981)

Experimental methods

Starting materials

Starting materials were samples of Mt. Hood andesite (MHA) and Goose Island basalt (GIB). Chemical analyses of these materials are presented in Table 1. The basalt is extremely iron-rich, containing over 17% (wt) FeO_t (total iron as FeO), and was selected in part because of the large anticipated weight change that would accompany a change of redox state. The chemistry and relationship of GIB to the Columbia River basalt stratigraphy has been discussed by Wright et al. (1973) and Helz (1978). The sample is from the uppermost of 2 flows near Ice Harbor Dam, Washington. Stratigraphically, these flows are near the top of the Upper Yakima series.

The MHA was selected as a contrasting composition with higher oxygen content and viscosity. The andesite contains approximately 5.5% (wt) FeO_t, hence the anticipated weight change in response to an imposed f_{O_2} is approximately 1/3 that for an equivalent amount of basalt. The relationship of the andesite to the geology of Mt. Hood has been described by Wise (1969).

Experimental apparatus and procedure

In this study the gain or loss of oxygen from the sample is used to determine the diffusion coefficient. The experimental design utilizes a high precision Cahn electrobalance to measure continuously sample weight change arising from the response of the sample redox state to an imposed f_{O_2}. The redox couple used to monitor the diffusion kinetics is the ferric-ferrous iron transition. One arm of the balance is suspended over the vertical tube of a Deltech gas-mixing furnace (Williams and Mullins 1981). The oxygen fugacity in the furnace is controlled by a $CO-CO_2$ mixture and measured using a ceramic oxygen electrolyte cell (Williams and Mullins 1976). The sample is suspended from a Pt support wire extending from the balance arm to within 1 cm of the ceramic oxygen electrolyte

cell (a distance of approximately 43 cm), the latter remaining in situ during the experiments. An inherent difficulty in monitering small weight changes at low f_{O_2} is the precipitation of graphite on the Pt support wire in the cooler portions of the furnace. To overcome this problem, the support wire is dropped through a 7 mm diameter ceramic tube (30 cm length), which is held at the top of the furnace tube by an O-ring seal, through which a slight positive pressure of Ar gas can be forced. By isolating the electrobalance in an Ar atmosphere with the only gas escape through the ceramic tube, the precipitation of graphite on the sample support wire is prevented.

The output systems of the electrobalance consist of a chart recorder (recording sample weight as a function of time), digital voltmeter displays which monitor the millivoltage corresponding to the oxygen fugacity and the balance output voltage, and an integrating printer which time averages the voltage inputs and prints sample weight and f_{O_2} as a function of time. Time-averaged data were collected at 10 min intervals except during the initial stages of high temperature experiments when the rate of sample weight change was high and data were collected at 2 min intervals. Signal noise is less than 10 μg when the atmosphere is pure CO_2 and less than 5 μg when the atmosphere is CO-rich. Total weight changes were about 0.5 mg for MHA and 1.5 mg for GIB.

Furnace temperature is controlled with a $Pt_{94}Rh_6-Pt_{70}Rh_{30}$ thermocouple located between the heating elements, outside the muffle tube. Temperatures are measured, however, with a $Pt\text{-}Pt_{90}Rh_{10}$ thermocouple within the ceramic oxygen electrolyte cell. A difference of 5° C exists between the temperature of the sample and that recorded in the cell; sample temperatures are reported in this paper. Temperatures are accurate to better than ±5° C and precise to ±1° C.

The samples were suspended on Pt wire (0.10 mm diameter) loops (method of Donaldson et al. 1975) attached to the Pt support wire. The loops had been previously "Fe-saturated" by running samples of the same approximate weight as the samples used in the diffusivity measurements at 1260° C and $\log f_{O_2} = IW + 0.5$ for a period of 24 h for the andesite and at 1160° C and $\log f_{O_2} = IW + 0.5$ for 25 h for the basalt. The silicate beads were then dissolved in HF acid and the loops reused in the diffusion experiments. Iron activities are not exactly matched over the range of f_{O_2} considered in this study; however, minimization of iron-loss to the Pt loops is indicated by observations that sample weights do not decrease with elapsed time of the experiment and by FeO analyses of the samples after the experiments (Table 1).

Experiments with a sample of GIB were made at 1160°, 1260°, and 1360° C and with MHA at 1260° and 1360° C. A second sample of basalt (GIB-2) was run at 1260° C. Sample weights for the basalt were 128 and 65 mg, respectively; the andesite sample weight was 148 mg. The liquidus of the basalt is 1115° C (Helz 1978) while that of the andesite is approximately 1250° C (Eggler and Burnham 1973). Samples were initially equilibrated at a given temperature and f_{O_2} until sample weight was constant and then cycled between f_{O_2}s of about IW+0.5 (log) and pure CO_2, the endpoints being about 7–8 log f_{O_2} units apart. Redox equilibria were approached from both oxidizing (weight gain) and reducing (weight loss) directions at 1160° C. Volatilization of components from the samples at 1260° and 1360° C and low oxygen fugacities, however, precluded reliable high temperature measurements in a reducing direction. All diffusion coefficients at 1260° and 1360° C are derived from experiments that were run in an oxidizing direction.

Table 1 includes partial analyses of the samples determined after the runs. For a run duration of 16 days (at 1260° and 1360° C), MHA lost 2% of its weight while the basalt lost 3.7% of its weight over 10 days (temperatures ranging from 1160° to 1360° C). Alkalies, and particularly Na, are volatilized. Similar observations have been reported by Donaldson (1979), Corrigan and Gibb (1979), and Seifert et al. (1979). Because previous studies have delineated a strong positive correlation between alkali content and oxygen diffusion coefficient (May et al. 1974; May and Wollast 1974), measurements were performed at 1160° C for the basalt and at 1260° C for the andesite both *before* and *after* all the higher temperature measurements were made. The anticipated decrease in diffusivity was not observed for either composition, suggesting that oxygen diffusion mechanisms in natural systems are considerably more complex than those in simple systems.

Analysis of data

The diffusion model is non-steady state: oxygen penetrates a sphere of uniform initial concentration from a constant and semi-infinite medium. The total amount of diffusing substance (oxygen) entering or leaving the sphere is described by the following solution to the diffusion equation:

$$(M_t/M_0 = 1-(6/\pi^2)\sum_{n=1}^{\infty} n^{-2}\exp(-n^2\pi^2 Dt/r^2) \quad (1)$$

(Crank 1975), where M_t and M_0 are the amounts of oxygen that have diffused into the sphere of radius r in time t and at infinite time, respectively, and D is the diffusion coefficient defined by Fick's Law. This diffusion equation is presented in terms amenable to thermogravimetric balance measurements. Because the entire range of fractional equilibration has been determined experimentally, the evaluation of D follows directly from balance measurements of weight change as a function of time if the radius of the sphere is known. It is assumed that only radial diffusion occurs and that D does not vary as a function of time.

One means of solving the equation given above is by plotting $\log [1-(M_t/M_0)]$ vs t and measuring the slope of the curve at large t when it approaches a straight line. As pointed out by Serin and Ellickson (1941), however, a straight line occurs when all the terms in the series become negligible compared to the first term. For a sphere, M_t/M_0 must be about 0.7 (or the diffusion process must be about 70% completed) for this to occur. Serin and Ellickson present an alternative method to circumvent this limitation in which a curve that relates M_t/M_0 to $\pi^2 Dt/r^2$, and that represents all the terms in the series, is calculated. Because a value of $\pi^2 Dt/r^2$ uniquely defines a value of M_t/M_0, knowing the value of t (and sample radius) for a given fractional saturation allows calculation of D. The method of Serin and Ellickson (1941) was adopted in this study because it allows Ds to be calculated for any and all data points. Calculated oxygen diffusivities were typically low for data points representing short elapsed times (an artifact that is related to changing the furnace f_{O_2}; discussed later), but rapidly attained a plateau value that was interpreted to be the true oxygen diffusion coefficient for the run conditions. These plateau values were averaged and a standard deviation calculated.

Figure 1 compares the derived oxygen diffusivity (line) to the experimental data (points) for a typical experiment. The validity of the analytical method is corroborated by the excellent agreement (with the exception of the point at short elapsed time). Additionally, when calculated oxygen diffusivities are substituted into Eq. (1) and the series expansion solved for fractional saturation, convergence to the experimental value is confirmed: convergence typically requires three or less terms for $t > 6000$ sec, five terms for $t = 1500$ sec, and greater than 10 terms for $t < 600$ sec.

The radii of the sample beads were determined from calculated melt densities (Bottinga and Weil 1970) using the analyses in Table 1 and assuming spherical sample geometry. These radii are 0.221 cm for GIB, 0.243 cm for MHA, and 0.177 cm for GIB-2. The uncertainties resulting from a calculated density are insignificant in relation to those arising from assuming a spherical geometry. For example, changing the density of MHA from 2.46 g/cm^3 to 2.51 g/cm^3 decreases the calculated bead radius by 0.0016 cm (for a sample weight of 148 mg) which affects the diffusivity by less than 1%. Because the change in radius due to the effect of thermal expansion on the molar volume (and density) is less than 0.001 cm over the temperature interval 1160°–1360° C, only the radius determined at 1260° C for each composition is used in calculating the diffusivity.

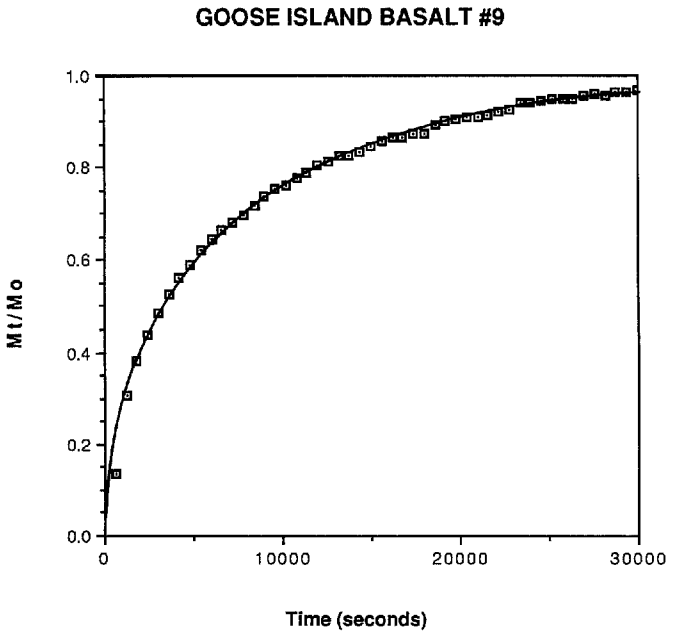

Fig. 1. Experimental measurements (*squares*) showing change in fractional saturation, M_t/M_0, of Goose Island basalt as a function of elapsed time (experiment 9; 1160° C). The *solid line* represents the calculated oxygen chemical diffusivity. Data were collected at 10 min intervals. The total weight change is approximately 1.5 mg

Aberration from spherical geometry can introduce appreciable errors of a systematic nature into the calculation: Because diffusivity varies as the square of the radius, an error of +10% increases D by about 20%. The GIB bead geometries, measured by micrometer, are slightly tear-drop shaped with a length (axis of rotation) to width ratio of approximately 5:4. The sample volume is the same (within the uncertainties), however, whether calculated from the Bottinga and Weill (1970) density or from the measured dimensions and the volume formula for a prolate spheroid. The bead of MHA was noticeably deformed during an attempt to fast quench and measurements of that sample geometry are not available. (Other experiments with MHA showed a tendency to form more spherical beads than the basalt, presumably because of the higher viscosity of the andesite). Although it is difficult to quantify the effect of sample shape on D, any deviation from sphericity will reduce the effective diffusion distance. Calculated Ds are, therefore, maximum values and may be systematically higher than true values.

In addition to the assumptions of spherical sample geometry and constant D as a function of time at a given temperature, it is also assumed that:

(1) the surface is brought to the equilibrium oxygen concentration instantaneously when the oxygen fugacity is changed; and

(2) the kinetics are diffusion controlled.

With regard to assumption (1), changing f_{O_2} from pure CO_2 to IW + 0.5 (log) takes approximately 3–4 min although the f_{O_2} is within 1 log unit of the desired atmosphere within 1 min. The reverse cycle is slightly slower with the f_{O_2} change being completed within 4–5 min but within 1 log unit of the desired value in 1–2 min. The apparent consequence of changing f_{O_2} is that diffusivities calculated for short elapsed times (less than 25% of the total equilibration time; see Fig. 1) are lower than those for long times. Dunn (1982) attributed similar observations to a competing transport process (other than oxygen diffusion) that is rate-limiting during the initial stages of experiments. This process, which he believed to be the establishment of a surface equilibrium between sample and furnace atmosphere, was observed to become negligible relative to the diffusion process as fractional saturation increased. The results of this study are consistent with Dunn's (1982) observations: calculated Ds rapidly increase to a constant value that is interpreted as the true oxygen diffusion coefficient for the run conditions.

With regard to the second assumption, it is difficult to establish that the rate controlling process is diffusion of oxygen, and not convection or a surface reaction and/or an internal reaction, because concentrations of the diffusing species as a function of distance have not been measured. There are four indirect lines of evidence, however, that support this assumption. First, the observed sample weight change suggests that oxygen is the diffusing component as opposed to another species such as CO_2. Given the initial GIB sample weight (128 mg), the FeO_t content (17.7 wt%), and assuming the oxidation reaction

$$2FeO + 1/2O_2 = Fe_2O_3 \quad (2)$$

occurs in the sample at run conditions, a maximum possible increase in basalt sample weight of 1.53 mg is predicted. Althoug it is not realistic to assume that reaction (2) goes to "completion" in either direction, this value is in close agreement with the observed change in sample weight (1.5 mg). The observed increase in the andesite sample weight on oxidation, about 1/3 that of the basalt weight increase, is commensurate with the different iron contents of the two samples. Additional evidence that diffusion is the rate-controlling process includes the experimental observation that calculated Ds are independent of sample size. The second sample of basalt, GIB-2, containing 1/2 the mass of the initial basalt sample, produced an oxygen diffusion coefficient that was indistinguishable from GIB-1. (This lack of dependence of calculated Ds upon sample size is an additional argument that volatilization and deviation from spherical geometry are not significant sources of error because surface area, which influences the former, and surface tension, which affects bead shape, are both functions of the mass of the bead.) Third, Semkow et al. (1982) determined experimentally that oxidation reactions for Co, Ni, and Zn in silicate (diopside) melts are many orders-of-magnitude more rapid than diffusion. Lastly, other investigators using similar experimental approaches (Dunn 1983; Schreiber et al. 1986), concluded that the determination of oxygen diffusivities by monitoring redox reactions in samples was indeed possible because oxygen diffusion was the rate-limiting process.

Experimental results

Oxygen diffusion coefficients for basalt and andesite melts at various temperatures are summarized in Table 2 and plotted in Fig. 2. Linear least-squares regression analysis of these data yields the following Arrhenius equations for the temperature dependence of D:

$$D = 36.4 \exp(-51{,}600 \pm 3200/RT) \text{ cm}^2/\text{s} \quad (3)$$

for the basalt, and

$$D = 52.5 \exp(-60{,}060 \pm 4900/RT) \text{ cm}^2/\text{s} \quad (4)$$

for the andesite. These equations have the general form:

$$D = D_0 \exp^{-E/RT} \quad (5)$$

where D_0 is the pre-exponential frequency factor, E is the activation energy (cal/mol), R is the gas constant (cal/deg-mol), and T is absolute temperature. Regression errors are calculated using the method of Birge (1932) and assuming a 1σ error in D.

Diffusion coefficients for GIB are approximately an order-of-magnitude greater than those for MHA. High diffusivities correlate with low melt viscosity, high ratios of non-bridging oxygens/tetrahedrally coordinated cat-

Table 2. Experimental results

Run no.	T (°C)	No. of points	$D_{oxygen} \pm 2\sigma$ (cm^2/s)
Goose Island basalt			
2-R	1160	13	$4.59 \pm 0.49 \times 10^{-7}$
3	1160	17	$5.47 \pm 1.37 \times 10^{-7}$
8-R	1160	14	$4.96 \pm 0.79 \times 10^{-7}$
9	1160	17	$4.64 \pm 0.62 \times 10^{-7}$
5	1260	17	$1.66 \pm 0.41 \times 10^{-6}$
6	1260	15	$1.81 \pm 0.33 \times 10^{-6}$
7a	1360	6	$4.48 \pm 0.55 \times 10^{-6}$
7b	1360	5	$4.54 \pm 0.48 \times 10^{-6}$
Goose Island basalt-2			
13	1260	7	$1.49 \pm 0.08 \times 10^{-6}$
Mt. Hood andesite			
4	1260	15	$1.37 \pm 0.14 \times 10^{-7}$
6	1260	28	$1.49 \pm 0.11 \times 10^{-7}$
11	1260	14	$1.44 \pm 0.26 \times 10^{-7}$
8	1360	11	$4.96 \pm 0.60 \times 10^{-7}$
10	1360	12	$4.64 \pm 0.63 \times 10^{-7}$

σ, standard deviation
2-R, 8-R are reversal experiments (oxygen loss)

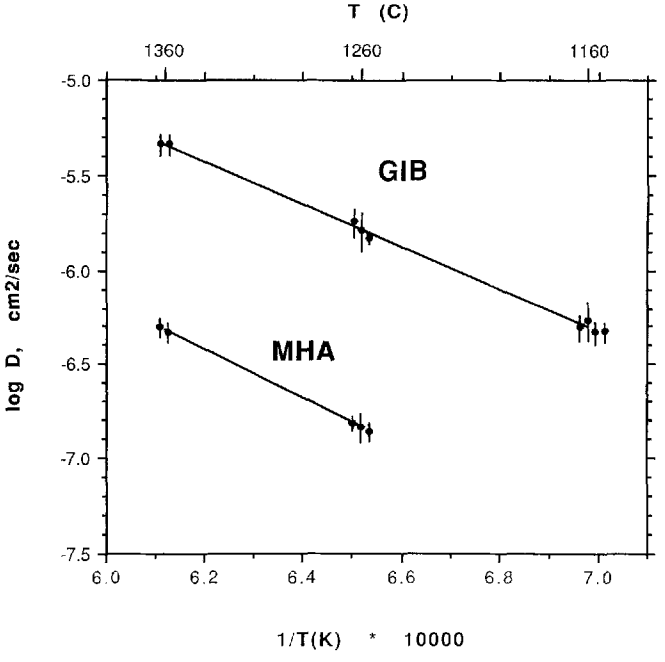

Fig. 2. Log_{10} of the diffusion rate for oxygen plotted against reciprocal absolute temperature for Mt. Hood andesite (MHA) and Goose Island basalt (GIB). Error bars are ± 2 standard deviations. *Lines* are least-squares fits

ions, NBO/T (Table 1; calculated using the procedure of Mysen et al. 1981), low initial oxygen content, and high contents of network modifying cations (Table 1).

The errors for the oxygen diffusion coefficients (Table 2) are reported at the two standard deviation level. These uncertainties are believed to be principally the result of the f_{O_2} instability and/or competing surface reaction that existed during the initial stages of each run. In general, the data are highly reproducible. Note, however, that although the temperature dependence relationship for MHA is based on 5 experiments, these experiments have been made at only 2 temperatures: sample volatilization at higher temperatures and initiation of crystallization at lower temperatures limited experiments to the range 1260°–1360° C. For these data, therefore, the Arrhenius activation energy is not well constrained.

Two of the data points at 1160° C for GIB were calculated from reduction experiments (weight loss) and two were determined from oxidizing experiments (weight gain). Inasmuch as the endpoints of the experiments differ by 7–8 $\log_{10} f_{O_2}$ units, the overlap of the data points, within statistical uncertainty, suggests that oxygen diffusivities are independent of f_{O_2} or the redox state of the melt. These data are believed to be the first reversed determinations of oxygen chemical diffusion coefficients in natural melts. Oxygen diffusivities in three basalt melts (Dunn 1983) and andesite melt (Dunn and Scarfe 1986) were based exclusively on reduction (oxygen loss) experiments. Canil and Muehlenbachs (1990) report that oxygen tracer diffusion coefficients are also independent of the redox state of the melt.

Discussion

Comparison with other data

Figure 3 compares the temperature dependence of D for the two compositions of this study with oxygen diffusion coefficients for other natural melts. Although the data are limited and varied with regard to the type of diffusion coefficient and conditions at which they were collected, several features stand out:

1. There is a large offset between the results for GIB and Dunn's tholeiite (line 4, Fig. 3). This difference is tentatively ascribed to pressure and compositional differences between the two sets of experiments. The effect of increasing pressure was shown by Watson (1979) to decrease the tracer diffusivity of calcium, a trend that would explain the observed offset if applicable to oxygen. Dunn (1983) and Dunn and Scarfe (1986) however, suggested a complex relationship between pressure and oxygen diffusivity that is different from that observed for cations. They found that Ds initially decrease and then increase in the 1–10 kb range. Dunn (1983) noted an abrupt decrease in D for the tholeiite over a narrow pressure range from 6 to 8 kb which he attributed to anionic disproportionation reactions in the melt. The net change in D with increasing pressure from 4 to 12 kb, however, is about half that required to reconcile the difference shown for the two tholeiites in Fig. 3. Alternatively, the offset in Ds may be attributable to compositional differences between the tholeiite and GIB, particularly total FeO (17% in GIB vs 12.5% in the tholeiite), MgO (about 4% in GIB vs 11.3% in the tholeiite), K_2O (1.28% in GIB vs 0.51% in the tholeiite), and P_2O_5 (1.77% in GIB vs 0.28% in the tholeiite).
2. The chemical diffusion coefficients for oxygen are 1–2 orders of magnitude greater than the tracer diffusivities.

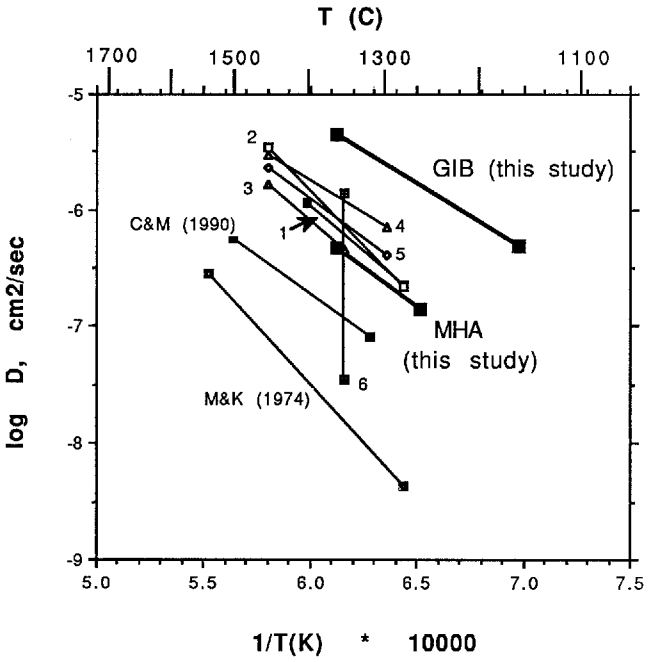

Fig. 3. Arrhenius plot comparing the results of this study with other oxygen diffusivities in natural silicate melts. M&K (1974) and C&M (1990) indicate 1 atm data of Muehlenbachs and Kushiro (1974) and Canil and Muehlenbachs (1990), respectively. *Lines (1)–(5)* are from Dunn (1983): *(1)*, *(2)*, and *(3)* are for alkali basalt at 4, 12, and 20 kbar, respectively; *(4)* is for 1921 Kilcaua tholeiite at 12 kb; and *(5)* is for Hamada nephelinite at 12 kbar. *Line (6)* is the pressure-dependent range (3.5–20 kb) for andesite (Dunn and Scarfe 1986)

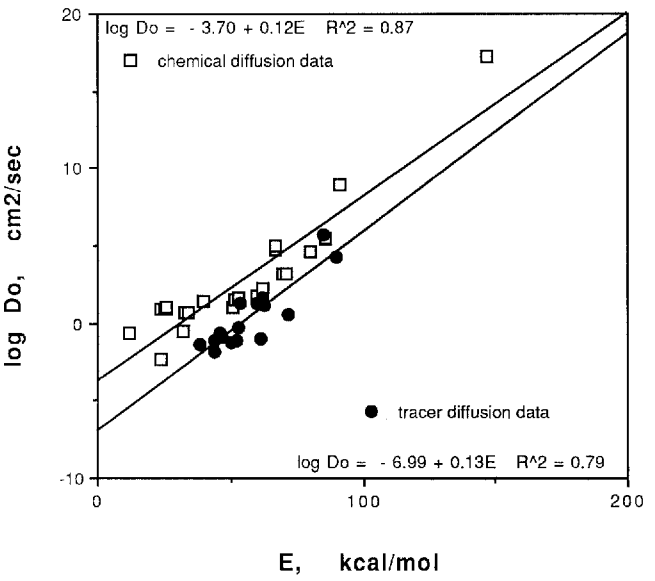

Fig. 4. Compensation law plot of the Arrhenius frequency factor, $\log_{10} D_0$, against the Arrhenius activation energy, E, for all known oxygen diffusion measurements in silicate melts (modified from Schreiber et al. 1986). *Solid lines* are least-squares fits. Chemical diffusion data (24 measurements) includes results of this study, Doremus (1960), Lawless and Wedding (1970), Sasabe and Goto (1974), Dunn (1983), Semkow and Haskin (1985), and Schreiber et al. (1986). Tracer diffusion data (17 measurements) include results of Koros and King (1962), May et al. (1974), Muehlenbachs and Kushiro (1974), Oishi et al. (1975), deBerg and Lauder (1978, 1980), Yinnon and Cooper (1980), Dunn (1982), Schaeffer et al. (1983), Shimizu and Kushiro (1984), and Canil and Muehlenbachs (1990)

This offset is consistent with predictions (Turkdogan 1983) and experiment (Schreiber et al. 1986) and has been related to differences in the diffusion mechanisms for oxygen that may involve predominantly molecular or neutral (chemical diffusion) versus ionic (tracer diffusion) species.

3. The activation energies for chemical diffusion are generally less than those for tracer diffusion. Although the data set is limited in extent, comparison of the 1 atm results in Fig. 3 illustrates this point. Muehlenbachs and Kushiro (1974) and Canil and Muehlenbachs (1990) determined activation energies of 90 and 60 kcal/mol which, on average, are substantially greater than the energies determined in this study, 51.6 and 60 kcal/mol. Muehlenbachs and Kushiro contended that the large observed activation energy indicated that tracer oxygen diffusion involved the breakage of Si–O bonds. Interestingly, the activation energy for alkali basalt at 12 kb (Dunn 1983), 86 kcal/mol, approaches the value reported by Muehlenbachs and Kushiro. Dunn argues, however, that this exceptional activation energy may be related to structural transformations involving the various anionic species in the melt at this particular pressure. Other investigators have noted the difference between chemical and tracer activation energies and proposed that tracer diffusion mechanisms may involve more extensive interactions between oxide ions, O^{2-}, and silicate and aluminosilicate anionic groups than chemical diffusion mechanisms (Turkdogan 1983; Schreiber 1986).

Chemical versus tracer diffusion

Evidence of different mechanisms for oxygen tracer and chemical diffusion stems from the systematic differences in observed diffusivities and activation energies. Specifically, chemical diffusion coefficients for oxygen are systematically higher than tracer diffusion coefficients, while their activation energies are systematically lower. Different mechanisms for the two types of diffusion are also indicated by separate compensation laws (for discussions of compensation, see Winchell 1969; Hart 1981). Figure 4, a compensation law plot of the frequency factor, D_0, versus the Arrhenius activation energy for all known oxygen chemical and tracer diffusion studies (selected irregardless of experimental methodology, physical and chemical state of the system, or measurement quality), shows a clear distinction between the two types of diffusion. The compensation law for oxygen chemical diffusion can be expressed as:

$$\log_{10} D_0 = 0.121E - 3.70 \; (r^2 = 0.87) \tag{6}$$

and for oxygen tracer diffusion as:

$$\log_{10} D_0 = 0.128E - 6.99 \; (r^2 = 0.79). \tag{7}$$

The statistically distinct compensations laws are interpreted as supporting different chemical versus tracer diffusion mechanisms. Relative to tracer diffusion, chemical diffusion changes less as a function of temperature

and is apparently easier to initiate, which may be related to a greater number of pathways available for diffusion. A previous attempt to define a compensation law relationship for oxygen combined tracer and chemical diffusivity data (Dunn 1982). This relationship, heavily biased by tracer diffusion data (and almost identical in slope and intercept to Eq. 7; see Fig. 4), was noted to be indistinguishable from Hofmann's (1980) general expression of the compensation law, based predominantly on cation diffusivities. Schreiber et al. (1986) first pointed out that the compensation law plot for chemical oxygen diffusion may not be the same as that for tracer oxygen diffusion, and they argued that separate compensation laws implied different diffusion mechanisms. Their conclusions are reinforced by the results of this study. Lowry et al. (1982) and Henderson et al. (1985) also used distinct compensation law relationships for alkalis to infer different diffusion mechanisms.

The results of this study are consistent with the theoretical and experimental observations of Schreiber et al. (1986) regarding the differences between oxygen chemical and tracer diffusion in silicate melts. Schreiber et al. argue that tracer diffusion involves *anionic oxygen* and a high degree of interaction with large, network-forming silicate and aluminosilicate anions and cite as evidence:
1. the determination of activation volumes for the diffusing species being about the size of the O^{2-} ion (Dunn 1983; Shimizu and Kushiro 1984);
2. qualitative solution of the Eyring equation relating experimental *D*s and melt viscosities when the effective diameter of the diffusing species is somewhat larger than the oxide anion dimension (perhaps the dimension of the SiO_4^{4-}-group; Yinnon and Cooper 1980; Dunn 1982; Shimizu and Kushiro 1984; and
3. similarity between the diffusion of tracer oxygen and divalent cations in the same systems (Dunn, 1982 1983).

Schreiber et al. note that the activation energy for tracer diffusion, although larger than that for chemical diffusion, is not sufficiently large to enable significant rupture of Si-O and Al-O bonds. The energies are, however, consistent with the movement of a free O^{2-} ion between discrete sites in a melt.

Chemical diffusion, on the other hand, is traditionally seen as involving the migration of *molecular oxygen*, either through channels or holes within the melt structure or via sequential exchanges with network oxygens (Schreiber et al. 1986), or *oxygen-bearing species* (silicate or aluminosilicate anions), coupled with back-diffusion of less oxygen-rich polymeric anions to prevent the development of Al and Si chemical potential gradients (Dunn and Scarfe 1986). It is not clear in the case of the latter proposed mechanism, however, why chemical diffusion of oxygen should be faster than tracer diffusion. Indeed, considering the dimensions of the diffusing charged particles, one would expect chemical diffusivities for oxygen to be less than tracer diffusivities, if this mechanism was valid.

An alternative mechanism, also consistent with existing experimental constraints, is that the weight change experiments measure diffusion of *vacancies* (E.B. Watson; personal communication 1990). According to this mechanism, when the oxygen fugacity around a melt droplet is lowered, oxygen atoms in the melt are lost to this atmosphere, each leaving a vacancy and (presumably 2) electrons. These vacancies diffuse down their concentration gradient (into the sample) by changing places with neighboring oxygens. Electrons also diffuse inward and are consumed by reaction with ferric iron. Because electrons probably move faster than vacancies, the overall process is probably rate-limited by vacancy diffusion. By this mechanism, individual oxygen atom transport over long distances is not required; a given oxygen atom has to make only one exchange for each diffusing vacancy. For the oxygen concentration to change at the center of the bead, therefore, it is only necessary that vacancies and some electrons get there. In contrast, tracer diffusion requires than a specific oxygen atom diffuse the entire distance from center to edge. A vacancy diffusion mechanism could operate equally well in response to an increase in the surrounding oxygen fugacity. A similar mechanism has been invoked for diffusion in olivine (Boland and Duba 1985). Turkdogan (1983) has documented the solution of oxygen into lattice vacancies in vitreous silica.

Diffusion distances for oxygen in silicate melts

If the diffusivity in a silicate melt is constant for a given temperature, then the "penetration distance" (the distance at which the concentration of diffusing substance is 50% of its final value) is approximately equal to $(Dt)^{1/2}$. Using this relationship, diffusion distances for oxygen in static magma bodies can be estimated: In one year, oxygen diffuses approximately 2.1 cm and 7.2 cm in andesite and basalt melts at 1260° C, respectively. In 10^6 years, diffusion distances are approximately 21.3 m for the andesite and 72.2 m for the basalt. The temperature dependence of these distances is, of course, exponential: for the basalt at 1160° C, oxygen diffuses 3.9 cm in a year, while at 1360° C the diffusion distance is 11.9 cm over the same period.

These calculations suggest that repose periods for melts at the surface or near surface are probably not sufficiently long for oxygen diffusion-controlled reactions (e.g., redox, assimilative melting) to be efficient. Because thermal diffusion is many orders-of-magnitude greater than chemical diffusion (Bowen 1921), and because *D* decreases exponentially with falling temperature, a static magma probably will not change its redox state to any measureable extent on eruption to the surface. Circulation of melt (e.g., convection, magma-mixing, magma replenishment, magma ascent) may be required to attain a particular equilibrium in melt at or near the surface. In the upper mantle or lower crust, however, repose periods may be significantly longer and diffusion-controlled redox processes may be important.

Application of the oxygen chemical diffusion coefficients in basalt and andesite melts from this study is dependent on whether the chemical potential gradient for oxygen is represented by a liquid-gas interface (similar to the experimental configuration) or by a liquid-solid

interface. The data are rigorously applicable only to the former case. To apply the data to the latter case, it must first be established that the interface reaction (crystallization, partial melting, assimilation) is fast, relative to the diffusion rate of oxygen and other components away from or towards the reaction surface. An important variable to consider in the application of the data to either case will be the ratio of reaction surface area to melt volume; that is, the geometry of the magma body.

Summary

Oxygen chemical diffusion coefficients for basaltic and andesitic melts have been determined as a function of temperature at 1 atm by monitoring the weight change associated with establishing redox equilibrium in these samples when oxygen fugacity is changed. Weight change was monitored continuously using a Cahn electrobalance. Observed oxygen diffusivities at 1160° to 1360° C are approximately an order-of-magnitude greater for the basalt than for the andesite, consistent with differences in viscosity, proportions of network modifying cations, and NBO/T in the two melts. Diffusivities at 1160° C for the basalt, obtained for reactions conducted in both oxidizing and reducing directions, confirm that oxygen diffusivity is independent of the redox state of the melt.

The compensation relationship for oxygen chemical diffusion is distinctly different from that for tracer diffusion. These different linear relationships are interpreted as supporting different diffusion mechanisms of oxygen. The lower Arrhenius activation energies and higher diffusivities associated with chemical diffusion support models for diffusion involving molecular oxygen or vacancies.

Acknowledgements. The work reported in this paper was done in the experimental petrology laboratory at the Johnson Space Center. Both samples were provided by Dr. G.E. Lofgren. Critical reviews of this manuscript at various times during its writing by Drs. J.B. Brady, T. Dunn, W.J. Harrison, A.W. Hofmann, and E.B. Watson are appreciated. The author is particularly appreciative of the contributions of Bruce Watson to understanding diffusion mechanisms. The author acknowledges the support of the Lunar and Planetary Institute which is operated by the Universities Space Research Association under contract with NASA.

References

Birge RT (1932) The calculation of errors by the method of least squares. Phys. Rev. 40:207–227

Boland JN, Duba A (1985) Defect mechanisms for the solid state reduction of olivine. In: Schock RN (ed) Point defects in minerals. Geophysical Monograph 31, AGU, pp 211–225

Bottinga Y, Weil DF (1970) Densities of liquid silicate systems calculated from partial molar volumes of oxide components. Am J Sci 269:169–182

Bowen NL (1921) Diffusion in silicate melts. J Geol 29:295–317

Canil D, Muehlenbachs K (1990) Oxygen diffusion in an Fe-rich basalt melt. Geochim Cosmochim 54:2947–2951

Corrigan G, Gibb FGF (1979) The loss of Fe and Na from a basaltic melt during experiments using the wire-loop method. Min Mag 43:121–126

Crank J (1975) The mathematics of diffusion, 2nd edn. Oxford Univ Press, London

Davis RF, Pask JA (1972) Diffusion and reaction studies in the system Al_2O_3-SiO_2. J Am Ceram Soc 55:525-531

deBerg KC, Lauder I (1978) Oxygen tracer diffusion in lead silicate glass above the transformation temperature. Phys Chem Glasses 19:78–82

deBerg KC, Lauder I (1980) Oxygen tracer diffusion in a potassium silicate glass above the transformation temperature. Phys Chem Glasses 21:106–109

Donaldson CH (1979) Composition changes in a basalt melt contained in a wire loop of $Pt_{80}Rh_{20}$: effects of temperature, time, and oxygen fugacity. Min Mag 43:115–119

Donaldson CH, Williams RJ, Lofgren GE (1975) A sample holding technique for study of crystal growth in silicate melts. Am Mineral 60:324–326

Doremus RH (1960) Diffusion of oxygen from contracting bubbles in molten glass. J Am Ceram Soc 43:655–661

Dunn T (1982) Oxygen diffusion in three silicate melts along the join diopside-anorthite. Geochim Cosmochim Acta 46:2293–2299

Dunn T (1983) Oxygen chemical diffusion in three basaltic liquids at elevated temperatures and pressures. Geochim Cosmochim Acta 47:1923–1930

Dunn T (1986) Diffusion in silicate melts. In: Scarfe CM (ed) Short course in silicate melts, vol 12. Mineral Assoc Canada, Ottawa, pp 57–92

Dunn T, Scarfe CM (1986) Variation of the chemical diffusivity of oxygen and viscosity of an andesite melt with pressure at constant temperature. Chem Geol 54:203–215

Eggler DH, Burnham CW (1973) Crystallization and fractionation trends in the system andesite-H_2O-CO_2-O_2 at pressures to 10 kb. Geol Soc Am Bull 84:2517–2532

Hart SR (1981) Diffusion compensation in natural silicates. Geochim Cosmochim Acta 45:279–291

Helz RT (1978) The petrogenesis of the Ice Harbor memeber Columbia Plateau, Washington: a chemical and experimental study. Ph D dissertation, Pennsylvania State University, USA

Henderson P, Nolan J, Cunningham GC, Lowry RK (1985) Structural controls and mechanisms of diffusion in natural silicate melts. Contrib Mineral Petrol 89:263–272

Hofmann AW (1980) Diffusion in natural silicate melts: a critical review. In: Hargraves RB (ed) Physics of magmatic processes. Princeton Univ Press, New Jersey, pp 385–417

Koros PJ, King TB (1962) The self diffusion of oxygen in a lime-silica-alumina slag. Trans Metal Soc AIME 224:299–306

Lawless WN, Wedding B (1970) Photometric study of the oxygen diffusivity in aluminosilicate glass. J Appl Phys. 41:1926–1929

Lowry RK, Henderson P, Nolan J (1982) Tracer diffusion of some alkali, alkaline-earth and transition element ions in a basaltic and an andesitic melt, and the implications concerning melt structure. Contrib Mineral Petrol 80:254–261

May HB, Wollast R (1974) Interdiffusion coefficients in SiO_2-K_2O melts. J Am Ceram Soc 57:30–34

May HB, Lauder I, Wollast R (1974) Oxygen diffusion coefficients in alkali silicates. J Am Ceram Soc 57:197–200

Muehlenbachs K, Kushiro I (1974) Oxygen isotope exchange and equilibration of silicates with CO_2 and O_2. Carnegie Inst Wash Yearb 73:232–236

Mysen BO, Virgo D, Kushiro I (1981) The structural role of aluminium in silicate melts – a Raman spectroscopic study at 1 atmosphere. Am Mineral 66:678–701

Oishi Y, Terai R, Ueda H (1975) Oxygen diffusion in liquid silicates and relation to their viscosity. In: Cooper AR, Heuer AH (eds) Mass transport phenomena in ceramics. Plenum Press, NY, pp 297–310

Sasabe M, Goto KS (1974) Permeability, diffusivity, and solubility of oxygen in liquid slag. Metal Trans 5:2225–2233

Schaeffer HA, Lachenmayr H, Pyc LD (1983) Oxdiation studies of amber glass. Glastech Ber 56K:602–607

Schreiber HD, Kozak SJ, Fritchman AL, Goldman DS, Schaeffer

HA (1986) Redox kinetics and oxygen diffusion in a borosilicate melt. Phys Chem Glasses 27:152–177
Seifert F, Virgo D, Mysen BO (1979) Sodium loss from sodium metasilicate melts in CO_2 and CO atmospheres. Carnegie Inst Wash Yearb 78:679
Semkow KW, Rizzo RA, Hskin LA, Lindstrom DJ (1982) An electrochemical study of Ni^{2+}, Co^{2+}, and Zn^{2+} ions in melts of composition $CaMgSi_2O_6$. Geochim Cosmochim Acta 46:1879–1889
Semkow KW, Haskin LA (1985) Concentrations and behavior of oxygen and oxide ion in melts of composition $CaO\text{-}MgO\text{-}xSiO_2$. Geochim Cosmochim Acta 49:1897–1908
Serin B, Ellickson RT (1941) Determination of diffusion coefficients. J Chem Phys 9:742–747
Shimizu N, Kushiro I (1984) Diffusivity of oxygen in jadeite and diopside melts at high pressures. Geochim Cosmochim Acta 48:1295–1303
Turkdogan ET (1983) Physicochemical properties of molten slags and glasses. Metals Society, London
Watson EB (1979) Calcium diffusion in a simple silicate melt to 30 kb. Geochim Cosmochim Acta 43:313–322
Wendlandt RF (1980) Oxygen diffusion in basalt and andesite melts. EOS 61:1142 (abstract)
Williams RJ, Mullins O (1976) A system using solid ceramic oxygen electrolyte cells to measure oxygen fugacities in gas-mixing systems. NASA TM X-58167
Williams RJ, Mullins O (1981) JSC systems using solid ceramic oxygen electrolyte cells to measure oxygen fugacities in gas-mixing systems. NASA TM-58234
Winchell P (1969) The compensation law for diffusion in silicates. High Temp Sci 1:200–215
Wise WS (1969) Geology and petrology of the Mt Hood area: a study of High Cascade volcanism. Geol Soc Am Bull 80:969–1006
Wright TL, Grolier MJ, Swanson DA (1973) Chemical variation related to the stratigraphy of the Columbia River basalt. Geol Soc Am Bull 84:371–386
Yinnon H, Cooper AR (1980) Oxygen diffusion in multicomponent glass forming silicates. Phys. Chem Glasses 21:204–211

Editorial responsibility: T. Grove